DOI: 10.19884/j.1672-5220.202305007

Design and Fabrication of Flexible Thermoelectric String-Based Fabrics

AHMAAD Hasib Ud Din[1,2], DU Minzhi[1,2], HAN Xue[1,2], JING Yuanyuan[1,2], YANG Xiaona[1,2], ZHANG Juan[1,2], CHEN Xinyi[1,2], SYED Rashedul Islam[1,2], HUANG Fuli[1,2], XU Jinchuan[1,2], ZHANG Kun[1,2*]

1. College of Textiles, Donghua University, Shanghai 201620, China
2. Key Laboratory of Textile Science & Technology, Ministry of Education, Donghua University, Shanghai 201620, China

Abstract: Flexible thermoelectric (TE) materials that convert heat into electricity have been widely used in wearable electronics and other flexible devices. In this work, inorganic TE pillars were combined with thermoplastic polyurethane (TPU) to assemble a flexible string-shaped TE generator (TEG) for the fabrication of the thermoelectric fabric (TEF). Moreover, finite element analysis (FEA) was used to optimize the dimensions of the TE string and evaluate its performance. The FEA results showed that the inter-pillar spacing significantly affected the temperature difference, the output voltage and the internal resistance. A maximum power density of 3.43 μW/cm^2 (temperate gradient ΔT = 10.5 K) was achieved by the TE string with a diameter of 3.5 mm and an inter-pillar spacing of 2 mm. However, under the experimental condition, the achievable power density of the fabricated three-dimensional (3D) TEF was limited to 29% of the simulation result because of the inclination of the TE string within the fabric concerning heat plate contact and copper wire-TE pillar connections. The actual TE string also demonstrated high flexibility and stable mechanical properties after 450 bending cycles. Thus, the study would provide a foundation for future research in developing more efficient TEFs to offer a comfortable and conformable option for wearable energy harvesting applications.

Key words: thermoelectric fabric (TEF); thermoelectric (TE) pillar; thermoplastic polyurethane (TPU); finite element analysis (FEA)

CLC number: TN377 **Document code**: A

Article ID: 1672-5220(2024)05-0474-08

Open Science Identity (OSID)

0 Introduction

The advancements in thermoelectric fabrics (TEFs) have shown promising potential for generating electricity from waste heat and powering wearable devices[1]. These fabrics offer convenience, sustainability, reliability, lightweight nature and integration capability with clothing and accessories. Previous research has explored various materials and techniques to combine electrical and thermal conductivities with flexibility for efficient energy conversion in flexible thermoelectric generators (TEGs), and facilitated their utilization in various flexible electronic industries, including entertainment, fitness, navigation and medical care[2-7]. Thin-film TEGs[8-9] utilizing p-type and n-type semiconductor materials have shown better flexibility. However, their efficiency and power output are significantly lower as compared to those of inorganic TEGs[10-14]. Likewise, three-dimensional (3D) printable composite materials[15] or structures[16] have been employed for 3D TEGs. However, their complex manufacturing processes make them challenging to implement in everyday electronic clothing production.

Textile-based TEGs represent a new class of wearable devices capable of generating electrical energy from body heat. Researchers have developed two-dimensional (2D) textile-based TEGs[17] and flexible TEGs with 3D architectures[18]. However, their high fabric thickness limits their integration into everyday clothing. 3D thermoelectric textiles (TETs) utilizing different fabric structures have achieved notable power densities. Researchers[19-20] have adopted a spacer fabric structure achieving a power density of 51.5 mW/m^2 at temperate gradient ΔT = 47.5 K and developed a stretchable, breathable and washable woven TET with a power density of 6.06 W/m^2 at ΔT = 80.0 K. Nevertheless, their large dimensions restrict their use in specific applications rather than conventional clothing, which impedes the development of electronic clothing[21] and various wearable devices[22].

In this work, the inter-spacing of the inorganic pillars has been optimized for power generation and flexibility. This optimization is performed within a specific thermoelectric (TE) string diameter to ensure their effective integration into TEFs. Finite element analysis

Received date: 2023-05-23

Foundation items: National Natural Science Foundation of China (No. 51973034); Natural Science Foundation of Shanghai, China (No. 23ZR1402500); Fundamental Research Funds for the Central Universities, China (Nos. 2232022G01 and 19D110106)

* Correspondence should be addressed to ZHANG Kun, email: kun.zhang@dhu.edu.cn

Citation: AHMAAD H U D, DU M Z, HAN X, et al. Design and fabrication of flexible thermoelectric string-based fabrics[J]. *Journal of Donghua University (English Edition)*, 2024, 41(5): 474-481.

(FEA) is utilized to determine the inter-pillar spacing between pillars for a fixed-diameter TE string. For the organic coating material, the authors choose thermoplastic polyurethane (TPU) due to its high stretchability[23] and low thermal conductivity[24]. Moreover, commercially available TE pillars are used for their easy availability and uniform thermoelectric properties.

1 Materials and Methods

1.1 Materials

Poly (dimethyl siloxane) (PDMS) and curing agent (Slygard™ 184) were purchased from Dow Corning Corp., Michigan, USA. Two pillars, p-type ($Bi_{0.5}Sb_{1.5}Te_3$) and n-type ($Bi_2Te_{2.4}Se_{0.6}$), were purchased from Wuhan Treasure In July Technology Co., Ltd., Wuhan, China. TPU Elastollan™ 1175AW was purchased from BASF, Shanghai, China. Dimethylformamide (DMF) was purchased from Sinopharm Group, Shanghai, China. All chemicals were used as received without further purification.

Spandex yarns (65 tex) and cotton yarns (40 tex) were purchased from Maixianxian, Shanghai, China.

1.2 FEA of TE strings

FEA was employed to determine the optimum inter-pillar spacing for a textile-based TEG with a fixed string diameter of 3.5 mm. The FEA was utilized to simulate the power density and the deformation of the TE string under bending loads. Solidworks 2021 was employed to design the TE string, as demonstrated in Fig. 1 (a). Ansys Workbench 19.2 was used to simulate the tested results. The pillar dimension in the yarn was 2.4 mm × 1.0 mm × 1.0 mm, as the target for the string was 3.5 mm. The electrode dimension was 2.5 mm × 1.0 mm × 0.1 mm. The length of the TE string was based on the inter-pillar spacing. The data for the materials was input into the simulation software according to Table A1 and Table A2 (Appendix). The results from the simulation were then used to identify the optimal inter-pillar spacing between the TE pillars.

1.2.1 Parameters for power generation simulation

In the optimization of inter-pillar spacing concerning deformation simulation setup, the upper plate was recognized as the hot surface and the lower plate was the cold surface to imitate the environment temperature, as shown in Figs. 1 (b) and 1 (d). The lower plate temperature was set to 296.0 K with convection heat transfer and the upper plate temperatures were set accordingly to temperature differences of 10.4, 6.4, 5.7, 2.4 and 1.2 K, respectively. To calculate the open circuit voltage, one side of the TEG was assigned a voltage of 0 V, as shown in Fig. 1 (c).

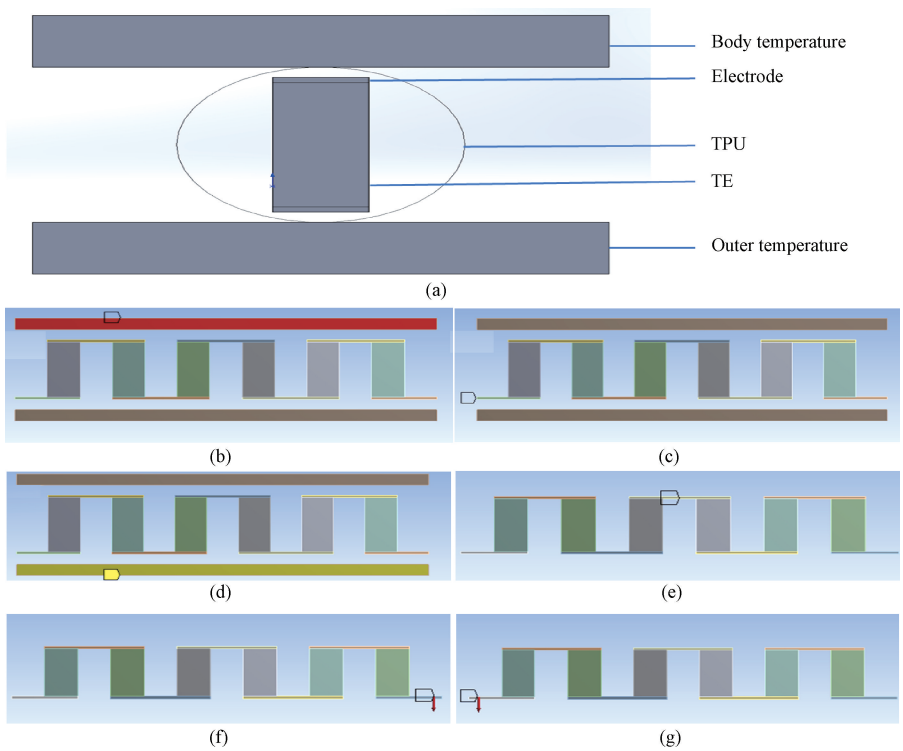

Fig. 1 Schematic diagram and boundary conditions for power generation and deformation for simulation: (a) design of TE string; (b) upper plate as variable hot-side temperature; (c) lower plate as fixed cold-side temperature; (d) voltage of 0 V to one surface of TEG; (e) fixed support in middle; (f)–(g) 2 N force applied on both sides

For measuring the internal resistance, another boundary condition was inserted by adding a voltage of 1 V from one side of the TEG and a current of 1 A on the other side of the TEG.

1.2.2 Parameters for deformation simulation

The pillar width was kept constant at 1 mm and the inter-pillar spacing was changed. Other parameters were the same as in Section 1.2.1 for the simulation. Moreover, fixed support was put in the middle with 2 N force on both sides for checking deformation, as shown in Figs. 1(e)–1(g).

1.3 Fabrication of TEFs

1.3.1 Preparation of TE strings

The TE strings were prepared through three steps as described below. The schematic diagram of the fabrication process is presented in Fig. 2.

1) DMF was employed as a solvent to dissolve the TPU pellets, achieving a TPU mass fraction of 30%. To ensure the full dissolution of TPU in DMF, magnetic stirring was utilized throughout the dissolution process, lasting approximately 2 h.

2) To achieve the desired shape and structure of the TE string, a 3D mold was employed. This mold was designed with software tools such as Cura 15.04.6 and Solidworks 2021. Polylactic acid (PLA) was used to construct the mold. A polarbear 3D+extended printer was used to create the mold. To prevent PLA from reacting with DMF, PLA was coated with a PDMS solution where the mass ratio of PDMS to the curing agent was 10∶1. The coated mold was dried for 48 h at room temperature, resulting in a smooth and durable surface ideal for molding the TE string.

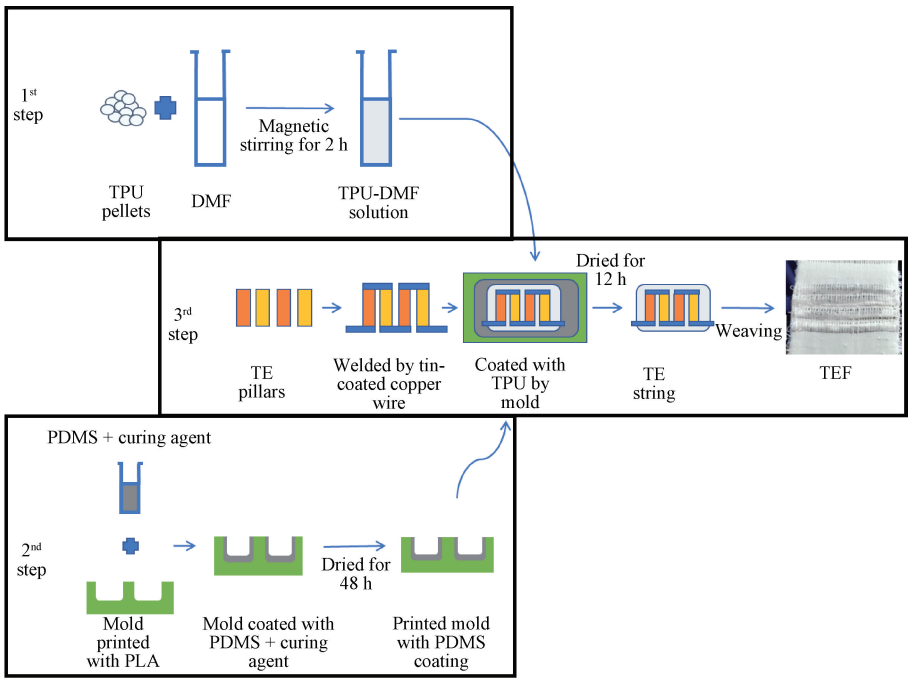

Fig. 2 Schematic diagram of TE string fabrication process

3) Tin-coated copper wire was joined with TE pillars via a welding process. The uniform spacing of TE pillars was ensured by incorporating an additional mold during the manufacturing process. This mold played a crucial role in maintaining consistent spacing between the TE pillars, which was a prerequisite for optimal device functioning. Subsequently, the TEG was carefully placed inside the PDMS-coated PLA mold, and the TPU-DMF solution was poured over it. The solution was left to sit in the mold for 12 h at room temperature, providing sufficient time for the evaporation of DMF. Once the evaporation process was completed, a tweezer was used to gently pull the TE string out of the mold.

1.3.2 Preparation of TEF

To produce the desired fabric for the research, a semi-automated sampling loom machine (SGA 568, Shanghai, China) was utilized. A 2/1 twill pattern was woven, with the TE strings positioned between four sets of commercially available spandex fibers, as shown in Fig. 3. For the warp yarn, a high-quality cotton yarn was selected, providing excellent durability and strength for the fabric. The weft yarn was spandex. By employing this approach, a TEF was successfully fabricated, which could potentially be used in wearable devices.

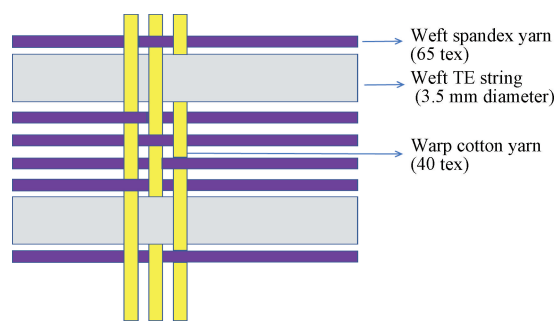

Fig. 3 TEF fabrication diagram

1.3.3 Characterization and measurements

A thermocouple (TES 1310, Shenzhen, China) was utilized to measure the temperature difference. A nanovoltmeter (Keithley 2182, Ohio, USA) was used to measure the voltage. A source meter (Keithley 2400, Ohio, USA) was used to create the temperature difference between the top and bottom sides of the TEF.

2 Results and Discussion

2.1 Simulation results and discussion

A linear relationship is observed between the inter-pillar spacing and the temperature difference (Fig. 4(a)), and between the inter-pillar spacing and the maximum output voltage (Fig. 4(b)). The underlying cause for this trend is attributed to the distance between the TE pillars. Specifically, as the distance between the PE pillars increases, more TPU is introduced, which possesses a lower thermal conductivity of 0.284 W/(m·K). This decrease in total thermal conductivity leads to an increase in the temperature difference between parallel electrodes. Furthermore, the open circuit voltage can be expressed as

$$V_{oc} = -S\Delta T, \quad (1)$$

where V_{oc} is the open circuit voltage; S is the Seebeck coefficient; ΔT is the temperature difference between heated electrodes.

The open circuit voltage also increases accordingly. For a TE pillar spacing of 2.2 mm, the maximum temperature difference and the maximum output voltage are determined to be 1.074 K and 0.001 3 V, respectively. A noticeable trend in the internal resistance of the TE string is observed in Fig. 4(c). The gradual increase in internal resistance is attributed to the increased length of the copper electrode with the increased inter-pillar spacing. This phenomenon can be explained by

$$R = \rho L/A, \quad (2)$$

where the resistance R is proportional to the length L and inversely proportional to the cross-sectional area A of the material. As such, an increase in the copper electrode length leads a consequent increase in resistance.

The power density of the TE string is illustrated in Fig. 4(e). As the inter-pillar spacing increases, the maximum power density decreases. The highest power density achieved is at the 1.2 mm inter-pillar spacing, which amounts to 3.88 $\mu W/cm^2$. A gradual increase in the maximum deformation of the TE string is observed in Fig. 4(d) when a 2 N force is applied at each end of the TE string and the fixed support is provided at the middle copper electrode. The deformation of the TE string is found to increase continuously as the inter-pillar spacing increases. This observation is attributed to the increasing mass of TPU in the fiber with the increasing of the inter-pillar spacing.

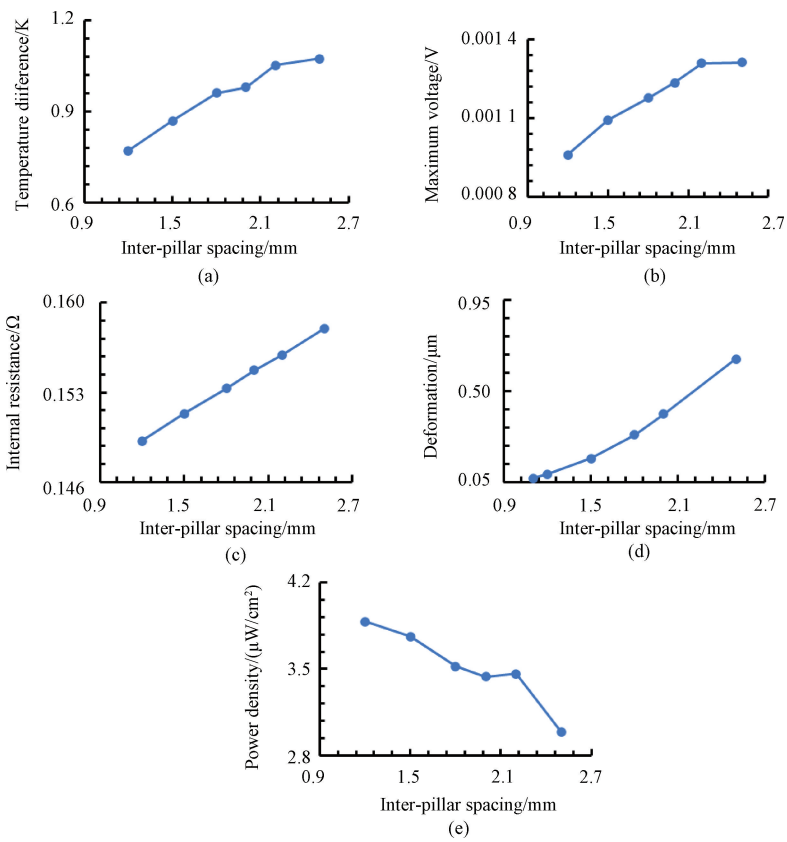

Fig. 4 Analyses of simulation results: (a) relation between inter-pillar spacing and temperature difference within TE strings; (b) relation between inter-pillar spacing and maximum output voltage; (c) relation between inter-pillar spacing and internal resistance; (d) relation between inter-pillar spacing and deformation; (h) relation between inter-pillar spacing and power density

The analysis revealed that increasing the inter-pillar spacing led to a decrease in the power density. However, it simultaneously raised the deformation and the flexibility of the TE string. Thus, if the aim was to generate a TE string with a power density of 3.88 μW/cm^2, creating an inter-pillar spacing of 1.2 mm would result in a very low deformation of only 0.087 μm, which would not qualify as a flexible string. Moreover, creating TE pillars with an inter-pillar spacing of 1.2 mm would pose a significant challenge for welding between the limited distanced TE pillars, making it impractical. Therefore, the inter-pillar spacing of 2.0 mm was selected, as it could achieve a power density of approximately 3.40 μW/cm^2 with a deformation of 0.400 μm. The simulation results of 2.0 mm inter-pillar spacing are shown in Fig. 5.

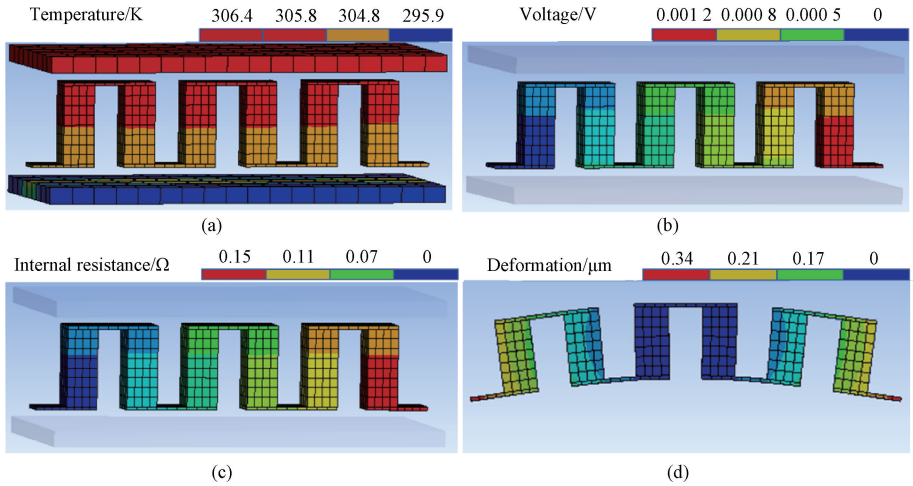

Fig. 5 FEA results with 2.0 mm inter-pillar spacing at ΔT = 10.5 K: (a) temperature difference within TE strings; (b) output voltage; (c) internal resistance; (d) deformation of TEF

2.2 Thermoelectric and mechanical properties of fabricated TEF

The open circuit voltage increases with the increasing of ΔT where the curve is constantly linear, as shown in Fig. 6 (a). To determine the power density, the voltage was measured across various external resistances using the same experimental setup. A peak in the voltage is observed at a resistance of approximately 10.5 Ω in Fig. 6 (b). An increase in the voltage resultes in a decrease in the short-circuit current, as illustrated in Fig. 6 (c). Moreover, the highest power density of 1.00 μW/cm^2 is obtained at this specific external resistance because the output power P reaches its maximum value when the internal resistance r of the TEG is equal to the external resistance R. The output power is calculated according to

$$P = \frac{U^2}{R + r}, \tag{3}$$

where U represents the output voltage. The TEF had a width of 2.2 cm and a length of 3.9 cm, and it was constructed using four pieces of TE strings. To assess the flexibility of the TEF, a bending test was examined. The resulting change in resistance ΔR was calculated as the difference between the resistance R after bending cycles and the original resistance R_0 without bending. Thus, $(\Delta R/R_0)\%$ represents the percentage change in resistance compared to the original resistance without bending. As illustrated in Fig. 6 (d), the TE string demonstrates remarkable mechanical flexibility as evidenced by the absence of significant resistance changes after 450 bending cycles. This can be attributed to the use of a TPU substrate, which is known for its flexibility and robustness. Figure 6 (d) illustrates the measurement of the bending radius, which yields a value of 5 mm.

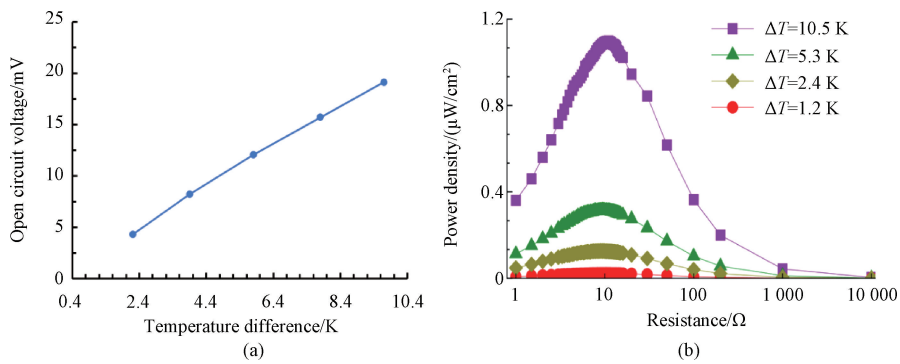

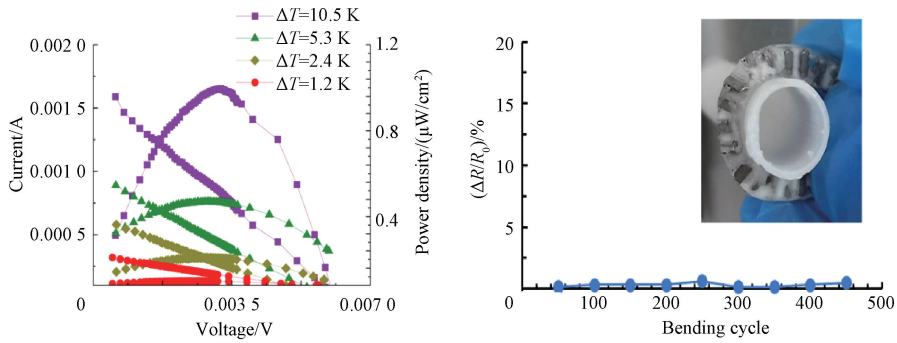

Fig. 6 Thermoelectric and mechanical properties of fabricated TEF: (a) open circuit voltage with respect to temperature difference; (b) power density with respect to resistance; (c) circuit current and power density as a function of output voltage; (d) stability of resistance with repetitive bending

The performance of the fabricated TEF is compared with the simulated result. The TEF has a power density of 1.00 μW/cm^2. However, according to the simulation data, the device is expected to operate at a power density of 3.43 μW/cm^2, as shown in Fig. 7 (a). This indicates that the fabricated TEF performs only 29% of the expected power density. There were several reasons for not achieving actual power density in the fabricated TEF compared to the simulation. Firstly, the inclination of the fiber to the hot and cold surfaces in the fabricated TEF differed from the simulation, where the hot and cold plates were flatly placed. This variation could affect the efficiency of the heat transfer. Secondly, the simulation only considered three pairs of TE pillars, neglecting the heat generated within the fabric that could not easily escape. By simulating a larger fabric, this additional heat could have been considered. Thirdly, in the simulation, the hot and cold surfaces were able to directly touch the heating surface, whereas, in the actual device, this direct contact was not possible due to the waviness of the TE string. This disparity could impact the heat transfer process. Lastly, the interconnection (welding) between TE pillars and electrodes was more challenging in this particular fabricated TEF due to the thinness of the yarn and the small size of the TE pillars. Human error during the welding process could have adversely affected the performance of the fabricated TEF.

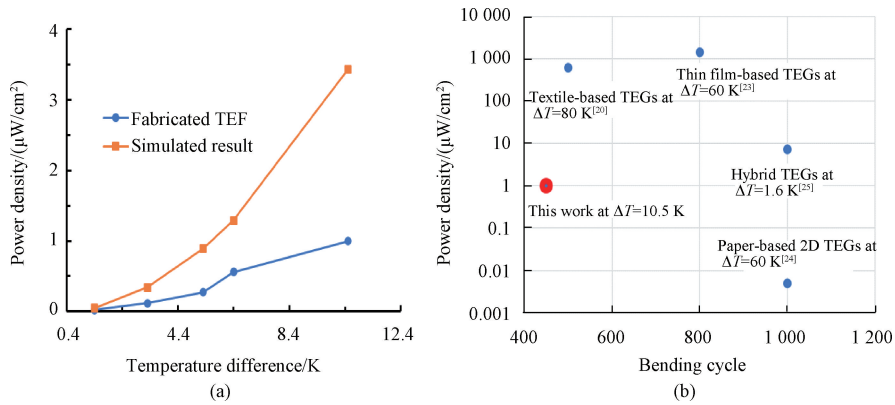

Fig. 7 Power density comparison: (a) comparison of fabricated TEF with the simulated result; (b) comparison of fabricated TEF in this work with that in published research work

Thin film-based TEGs shows enough power generation of 1 420 μW/cm^2 with good bending cycle properties[25] whereas paper-based TEGs[26] and hybrid TEGs[27] exhibit good flexibility with less power generation, as depicted in Fig. 7 (b). The highest textile-based TEGs reveals a power generation of 606 μW/cm^2 at a temperature difference of 80.0 K[20] which could be a milestone for this sector. Even though power generation is 1.00 μW/cm^2 at a temperature difference of 10.5 K in this work, it possesses moderate performance compared to other recent advancements. Moreover, the performance of the presented TEF is comparable to that of the hybrid TEGs with a minimum temperature difference. Furthermore, the small diameter of this TE string with high power generation capacity preserves its novelty among the published research results.

3 Conclusions

In this work, a TEF with optimal dimensioned TE strings and organic-inorganic material ratios was fabricated to have more power density as well as good flexibility and mechanical properties. This novel approach was to get assistance from the FEA and then fabricate the

yarn as well as the smart fabric. The fabricated TEF generated a power density of 1.00 $\mu W/cm^2$ at a temperature difference of 10.5 K, whereas the FEA simulation had predicted a required power density of 3.43 $\mu W/cm^2$ for efficient operation. This comparison revealed that the fabricated TEF achieved a performance level with a power density that was merely 29% of the simulated value. Nonetheless, this research significantly contributes to the advancement of a systematic TEF design.

References

[1] TOHIDI F, GHAZANFARI HOLAGH S, CHITSAZ A. Thermoelectric generators: a comprehensive review of characteristics and applications[J]. *Applied Thermal Engineering*, 2022, 201: 117793.

[2] YANG T T, XIE D, LI Z H, et al. Recent advances in wearable tactile sensors: materials, sensing mechanisms, and device performance [J]. *Materials Science and Engineering R: Reports*, 2017, 115: 1-37.

[3] WANG X W, LIU Z, ZHANG T. Flexible sensing electronics for wearable/attachable health monitoring [J]. *Small*, 2017, 13 (25): 1602790.

[4] SNYDER G J, TOBERER E S. Complex thermoelectric materials[J]. *Nature Materials*, 2008, 7: 105-114.

[5] LIU H, QING H, LI Z, et al. Paper: a promising material for human-friendly functional wearable electronics[J]. *Materials Science and Engineering R: Reports*, 2017, 112: 1-22.

[6] CAO T Y, SHI X L, CHEN Z G. Advances in the design and assembly of flexible thermoelectric device[J]. *Progress in Materials Science*, 2023, 131: 101003.

[7] SAEED M, SEAMUS O, AMIR P. Organic-based flexible thermoelectric generators: from materials to devices[J]. *Nano Energy*, 2022, 92: 106774.

[8] GUO Z P, YU Y D, ZHU W, et al. Kirigami-based stretchable, deformable, ultralight thin-film thermoelectric generator for BodyNET application [J]. *Advanced Energy Materials*, 2022, 12(5): 2102993.

[9] ELEONORA I, JACOB A, UBAIDAH S, et al. Towards low cost and sustainable thin film thermoelectric devices based on quaternary chalcogenides [J]. *Advanced Functional Materials*, 2022, 32(32): 2202157.

[10] VENKATASUBRAMANIAN R, SIIVOLA E, COLPITTS T, et al. Thin-film thermoelectric devices with high room-temperature figures of merit[J]. *Nature*, 2001, 413: 597-602.

[11] LIU H Y, WANG Y C, MEI D Q, et al. Design of a wearable thermoelectric generator for harvesting human body energy [C]//Wearable Sensors and Robots. Singapore: Springer, 2017: 55-66.

[12] KIM S J, LEE H E, CHOI H, et al. High-performance flexible thermoelectric power generator using laser multiscanning lift-off process [J]. *ACS Nano*, 2016, 10(12): 10851-10857.

[13] WANG Y, HONG M, LIU W D, et al. $Bi_{0.5}Sb_{1.5}Te_3$/PEDOT: PSS-based flexible thermoelectric film and device [J]. *Chemical Engineering Journal*, 2020, 397: 125360.

[14] YANG Y, HU H J, CHEN Z Y, et al. Stretchable nanolayered thermoelectric energy harvester on complex and dynamic surfaces[J]. *Nano Letters*, 2020, 20(6): 4445-4453.

[15] TZOUNIS L, PETOUSIS M, GRAMMATIKOS S, et al. 3D printed thermoelectric polyurethane/multiwalled carbon nanotube nanocomposites: a novel approach towards the fabrication of flexible and stretchable organic thermoelectrics [J]. *Materials*, 2020, 13(12): 2879.

[16] KIM S J, WE J H, CHO B J. A wearable thermoelectric generator fabricated on a glass fabric [J]. *Energy & Environmental Science*, 2014, 7(6): 1959-1965.

[17] CAO Z, TUDOR M J, TORAH R N, et al. Screen printable flexible BiTe-SbTe-based composite thermoelectric materials on textiles for wearable applications[J]. *IEEE Transactions on Electron Devices*, 2016, 63(10): 4024-4030.

[18] CHOI J, JUNG Y, YANG S J, et al. Flexible and robust thermoelectric generators based on all-carbon nanotube yarn without metal electrodes [J]. *ACS Nano*, 2017, 11(8): 7608-7614.

[19] ZHENG Y Y, ZHANG Q H, JIN W L, et al. Carbon nanotube yarn based thermoelectric textiles for harvesting thermal energy and powering electronics [J]. *Journal of Materials Chemistry A*, 2020, 8(6): 2984-2994.

[20] ZHENG Y Y, HAN X, YANG J W, et al. Durable, stretchable and washable inorganic-based woven thermoelectric textiles for power generation and solid-state cooling[J]. *Energy & Environmental Science*, 2022, 15 (6): 2374-2385.

[21] ZHANG R Q, LI D J, DU L J, et al. Design and weaving of flexible fabric connection for electronic clothing[J]. *Technical Textiles*, 2014, 32(2): 13-15, 19. (in Chinese)

[22] BAI Y F, XIE E X, LI Q, et al. Fabrication and characterization of yarn-based temperature sensor for respiratory monitoring [J]. *Journal of Donghua University (English Edition)*, 2022, 39 (6): 527-532.

[23] ELLEUCH R, ELLEUCH K, SALAH B, et al. Tribological behavior of thermoplastic polyurethane elastomers [J]. *Materials and*

Design, 2007, 28(3): 824-830.
[24] KOJIO K, FURUKAWA M, NONAKA Y, et al. Control of mechanical properties of thermoplastic polyurethane elastomers by restriction of crystallization of soft segment[J]. *Materials*, 2010, 3(12): 5097-5110.
[25] AO D W, LIU W D, ZHENG Z H, et al. Assembly-free fabrication of high-performance flexible inorganic thin-film thermoelectric device prepared by a thermal diffusion[J]. *Advanced Energy Materials*, 2022, 12(42): 2202731.
[26] ZHAO X, HAN W J, ZHAO C S, et al. Fabrication of transparent paper-based flexible thermoelectric generator for wearable energy harvester using modified distributor printing technology[J]. *ACS Applied Materials & Interfaces*, 2019, 11(10): 10301-10309.
[27] SUAREZ F, PAREKH D P, LADD C, et al. Flexible thermoelectric generator using bulk legs and liquid metal interconnects for wearable electronics[J]. *Applied Energy*, 2017, 202: 736-745.

Appendix

Table A1 TE properties of the materials used in the experiment

Material	Seebeck coefficient $S/(\mu V \cdot K^{-1})$	Thermal conductivity $K/(W \cdot m^{-1} \cdot K^{-1})$	Electrical conductivity $\sigma/(S \cdot cm^{-1})$
p-type pillars ($Bi_{0.5}Sb_{1.5}Te_3$)	200−205	1.35	950−1 050
n-type pillars ($Bi_2Te_{2.4}Se_{0.6}$)	210−230	1.65	950−1 050
Electrode (copper)	1.5	401	1.0×10^7
TPU	—	0.284	—
Air	—	0.002 42	—

Table A2 Mechanical properties of other materials used in the simulation software

Material	Density $\rho/(g \cdot cm^{-3})$	Tensile yield strength σ_y/MPa	Tensile strength σ_u/MPa
Copper	8.94	33.5	152
TE pillars	7	255	460
TPU	0.031 9	0.004 14	0.145

柔性条状基热电织物的设计及织造

AHMAAD Hasib Ud Din[1,2], 杜敏芝[1,2], 韩　雪[1,2], 景媛媛[1,2], 杨晓娜[1,2], 张　娟[1,2], 陈馨逸[1,2], SYED Rashedul Islam[1,2], 黄夫力[1,2], 徐金川[1,2], 张　坤[1,2*]

1. 东华大学 纺织学院, 上海 201620
2. 东华大学 纺织面料技术教育部重点实验室, 上海 201620

摘　要: 可将热量转化为电能的柔性热电（thermoelectric, TE）材料已广泛应用于可穿戴电子设备和其他柔性设备中。该研究将无机 TE 柱与热塑性聚氨酯（thermoplastic polyurethane, TPU）结合, 组装成柔性条状热电器（thermoelectric generator, TEG), 进一步用于热电织物（thermoelectric fabric, TEF）的织造。采用有限元分析（finite element analysis, FEA）优化柔性 TE 条的尺寸并评估其性能。FEA 的结果显示, TE 条的间距对温差、输出电压和内阻有显著影响。当 TE 条直径为 3.5 mm、条间距为 2.0 mm 时, 可获得最大功率密度, 达到 3.43 μW/cm^2（在温差 $\Delta T = 10.5$ K 的条件下)。在试验条件下, 热板接触以及铜线−TE 条连接处存在倾斜, 导致所织造的三维 TEF 的功率密度只能达到模拟结果的 29%。尽管如此, 在经过 450 次弯曲测试后, TE 条仍展现出优异的柔韧性和稳定的机械性能。这一研究不仅为今后开发更高效的 TEF 奠定了基础, 还为可穿戴式能量采集应用提供了更加舒适、合身的选择方案。

关键词: 热电织物（TEF); 热电柱（TE 柱); 热塑性聚氨酯（TPU); 有限元分析（FEA）